Atom Probe Tomography Analysis of the Local Chemical Environment at the Austenite/Ferrite Interfaces of Cast Duplex Stainless Steels*

Sarah Mburu[1], R. Prakash Kolli[1], Daniel E. Perea[2], Samuel C. Schwarm[1], Arielle Eaton[2], Jia Liu[2], Shiv Patel[1], Jonah Bartrand[2], and Sreeramamurthy Ankem[1]

[1]Department of Materials Science & Engineering, University of Maryland (UMD), College Park, Maryland 20742
[2]Environmental Molecular Sciences Laboratory (EMSL), Pacific Northwest National Laboratory (PNNL), Richland, WA 99352

***Abstract*– Cast duplex stainless steel piping in light water reactors experience thermal aging embrittlement during service at elevated temperatures. Interest in extending the service life to 80 years requires an increased understanding of the microstructural evolution and corresponding changes in mechanical behavior. We characterized the statically cast CF–3 and CF–8 stainless steels employing state-of-the-art atom-probe tomography (APT). The microstructure and mechanical properties of the steels that are isothermally aged to 4300 h at 400 °C are compared to the unaged steels. The results illustrate that spinodal decomposition, G–phase precipitation, carbide formation, and interfacial segregation of elements between phases influence thermal aging embrittlement.**

***Keywords*-- spinodal decomposition, duplex stainless steel, atom probe tomography, $M_{23}C_6$ carbide, chemical partitioning**

I. Introduction

Cast duplex stainless steels (CDSS) are used in cooling water piping of light water reactors (LWRs) due to their combination of strength, good ductility, good impact toughness, corrosion resistance, castability and weldability. We have characterized the mechanical properties and the microstructure of statically cast CF–3, [Fe, 0.02 C, 1.07 Mn, 0.98 Si, 19.69 Cr, 8.4 Ni, 0.28 Mo (wt.%)], and CF–8, [Fe, 0.06 C, 0.99 Mn, 0.97 Si, 19.85 Cr, 8.3 Ni, 0.35 Mo (wt.%)] steels at multiple length scales, employing state-of-the-art atom-probe tomography (APT) and energy-dispersive x-ray spectroscopy (EDS) for chemical analysis at finer scales. The steels have a duplex microstructure of face-centered cubic (f.c.c.) γ–austenite and body-centered cubic (b.c.c.) δ–ferrite phases. The ferrite phase is present in volume fractions less than approximately 13%. These alloys experience thermal aging embrittlement during operational service due to spinodal decomposition of the δ–ferrite phase into chromium-rich (Cr-rich) α'–domain and iron-rich (Fe-rich) α–domain, and nucleation and growth of intermetallic nickel-silicides G–phase precipitates [1], [2]. Microstructural evolution and concomitant changes in macroscopic (bulk) mechanical properties lead to increased hardness, a loss of ductility, and a reduction in impact toughness. Interest in extending the operational life of these power plants to 80 years requires examining the complex phase decomposition and corresponding mechanical property changes of these stainless steels by employing accelerated isothermal aging at elevated temperatures, e.g. 400 °C, relative to the operational temperatures. This requires detailed compositional characterization of the unaged stainless steels in order to provide a baseline reference to quantify the temporally evolving concentration profiles and phase decomposition at the different temperatures. Additionally, the γ–austenite/δ–ferrite heterophase interface must be characterized, as possible heterogeneous nucleation and growth of intermetallic precipitates or carbides at this location will significantly influence the local elemental concentration profiles and bulk mechanical properties.

II. Methodology

Figure 1 partially depicts the experimental flowchart. Mechanical properties from tensile tests, Charpy impact tests, Vickers Micro-hardness tests, and Nanoindentation measurements were performed in accordance with their respective ASTM standards. Volume fractions were measured from optical microscopy. Chemical analysis was performed by EDS and APT, where the concentration profiles were derived from proximity histogram of a 4.5 at.% Ni isoconcentration surface at the heterophase interface. The elemental concentrations of individual phases were derived from integrated counts of the EDS spectra from scanning electron microscope (SEM) and Transmission electron microscope (TEM). Specimens with a needle-shaped geometry necessary for APT analysis were fabricated using a FEI Helios dual-beam focused ion beam in the SEM (SEM/FIB) instrument following standard lift-out and sharpening procedures [3] as shown in Fig. 2.

III. Results and Discussion

Table 1 shows the ferrite, austenite, and carbide concentrations. Chemical mapping by EDS and APT illustrated chemical partitioning of Cr to the ferrite phase and Fe & Ni to the austen-

Manuscript received April 1, 2015; revised May 15, 2015 and June 1, 2015; accepted July 1, 2015. Date of publication July 10, 2015; date of current version July 31, 2015.
Corresponding author: S. Mburu (e-mail: smburu@umd.edu).
Color versions of one or more of the figures in this paper are available online at http://ieeexplore.ieee.org.
Digital Object Identifier (inserted by IEEE).

* This work is supported by the Department of Energy (DOE) Nuclear Energy University Programs (NEUP), contract number DE-NE0000724. Ms. Mburu is partially supported by the National Science Foundation (NSF) Louis Stokes Alliances for Minority Participation (LSAMP) under Grant No. 0833018. Mr. Schwarm is supported by Department of Energy: Office of Nuclear Energy (DOE-NE) Integrated University Program (IUP) fellowship program.

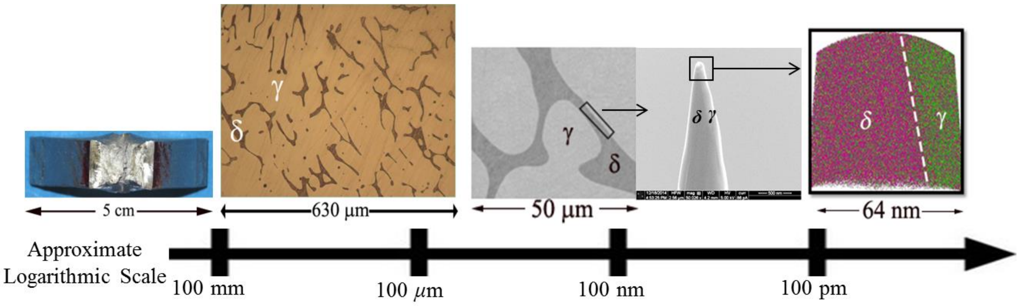

Fig. 1. Experimental procedures across multiple length scales leading to atomic level analysis: APT reconstruction of unaged CF–3, depicting 30% of the Cr ions (magenta), and 100% of Ni (green) and C (black) ions for clarity.

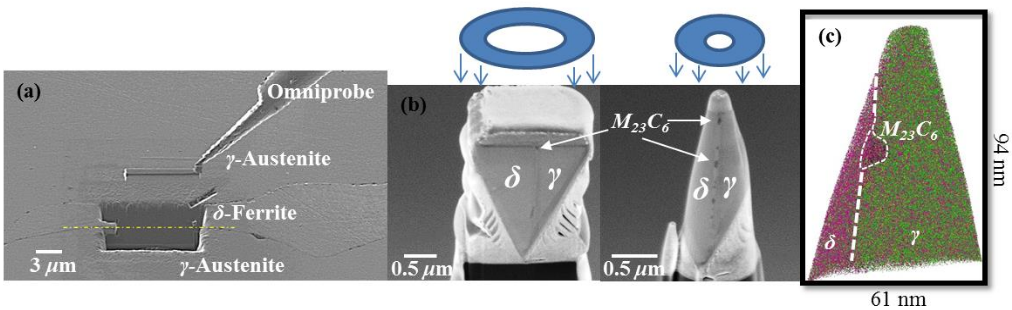

Fig. 2. (a) The *in situ* site-specific lift-out of an APT sample at the *δ*–ferrite/*γ*–austenite heterophase interface (dashed yellow line) using a SEM/FIB instrument. (b) Series of images illustrating annular milling of a specimen into needle morphology with subsequently decreasing tip diameter necessary for APT analysis. (c) The APT reconstruction of unaged CF–8, depicting 30% of the Cr ions (magenta), and 100% of Ni (green) and C (black) ions for clarity.

TABLE 1
COMPOSITIONS (at. %) OF PHASES IN APT SPECIMENS

		Ferrite		Austenite		Carbide		G–phase		
		Cr	Ni	Cr	Ni	Cr	C	Ni	Si	Mn
Unaged	CF–3	29	3.5	23	8.5	NA[a]		NA		
	CF–8	25	3	23	8.5	49	12	NA		
400 °C	CF–3	28.5	3.5	23	8.5	NA		23	8	7
	CF–8	27	4	23	8.5	-		24	8	9

[a] Not Applicable

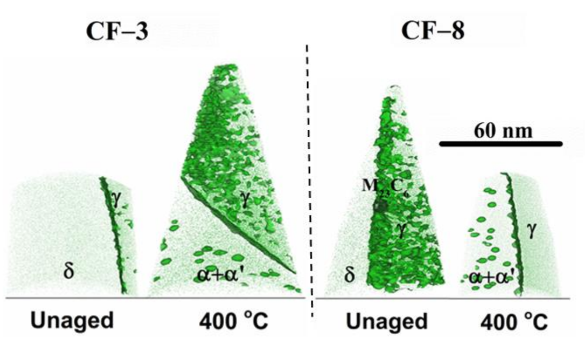

Fig. 3. The APT reconstructions of CF–3 and CF–8 steels' ferrite phase that are unaged (δ) and thermally aged (α+α') to 4300 hours at 400 °C illustrate G–phase precipitates in the aged samples.

ite phase. The carbide at the CF–8 heterophase interphase is enriched in C and Cr, which causes a local depletion of Cr in the ferrite phase. There is synergy between the carbide and spinodal decomposition in the ferrite phase of the unaged CF–8 steel because the carbides locally deplete the ferrite phase of Cr – one of the two elements involved in diffusion during spinodal decomposition, as discussed above. Correlative TEM studies confirmed the Cr depletion zone in the ferrite phase and the presence of f.c.c. superlattice diffraction spots is indicative of a $M_{23}C_6$ carbide phase. The *γ*–austenite phase is not affected during aging to 4300 h. The CF–3 steel, with three times less carbon than CF–8, does not have carbides. Figure 3 and Table 1 show that G–phase precipitates, as represented with 5.5 at.% Ni isoconcentration surfaces, exist only in aged samples for both alloys.

IV. CONCLUSIONS

There is a trend for lower impact toughness with corresponding higher yield strength, tensile strength and hardness as the steels are thermally aged. The carbides in CF–8 also provide solid-solution strengthening as compared to CF–3. Spinodal decomposition was observed in the unaged and aged steels. As spinodal progresses, more chemical partitioning occur in the ferrite to form G–phase precipitates.

ACKNOWLEDGMENT

We would like to thank Mr. Michael Perna at UMD for machining all specimens and the support of Lloyd Lab and MEMIL Lab for testing mechanical properties. We acknowledge the use of SEM/TEM at the University of Maryland NanoCenter and its AIMLab and FabLab facilities. The APT was performed using EMSL, a DOE Office of Science User Facility sponsored by the Office of Biological and Environmental Research and located at Pacific Northwest National Laboratory.

REFERENCES

[1] F. Danoix and P. Auger, "Atom Probe Studies of the Fe–Cr System and Stainless Steels Aged at Intermediate Temperature: A Review," *Mater. Charact.*, vol. 44, no. 1–2, pp. 177–201, Jan. 2000.

[2] H. M. Chung and T. R. Leax, "Embrittlement of laboratory and reactor aged CF3,CF8, and CF8M duplex stainless steels," *Mater. Sci. Technol.*, vol. 6, no. 3, pp. 249–262, Mar. 1990.

[3] K. Thompson, D. Lawrence, D. J. Larson, J. D. Olson, T. F. Kelly, and B. Gorman, "In situ site-specific specimen preparation for atom probe tomography," *Ultramicroscopy*, vol. 107, no. 2–3, pp. 131–139, Feb. 2007.